Earth and Planetary Science Letters 269 (2008) 554–564

Contents lists available at ScienceDirect

Earth and Planetary Science Letters

journal homepage: www.elsevier.com/locate/epsl

An integrated stratigraphic record from the Paleocene of the Chijiang Basin, Jiangxi Province (China): Implications for mammalian turnover and Asian block rotations

William C. Clyde [a,*], Yongsheng Tong [b], Kathryn E. Snell [c], Gabriel J. Bowen [d], Suyin Ting [e], Paul L. Koch [c], Qian Li [b], Yuanqing Wang [b], Jin Meng [f]

[a] Department of Earth Sciences, University of New Hampshire, James Hall, 56 College Rd., Durham, NH, 03824, United States
[b] Institute of Vertebrate Paleontology and Paleoanthropology, Chinese Academy of Sciences, P.O. Box 643, Beijing 100044, PR China
[c] Department of Earth and Planetary Sciences, University of California, Santa Cruz, CA 95064, United States
[d] Department of Earth and Atmospheric Sciences, 550 Stadium Mall Drive, Purdue University, West Lafayette, IN 47907, United States
[e] Museum of Natural Science, Louisiana State University, Baton Rouge, LA 70803, United States
[f] Department of Vertebrate Paleontology, American Museum of Natural History, New York, N.Y 10024, United States

ARTICLE INFO

Article history:
Received 1 December 2007
Received in revised form 29 February 2008
Accepted 3 March 2008
Available online 15 March 2008

Editor: H. Elderfield

Keywords:
Paleocene
mammals
China
paleoclimate
stratigraphy
paleomagnetism

ABSTRACT

New paleomagnetic and isotopic results from a ~1000 meter thick Paleocene stratigraphic section in the Chijiang Basin of China's Jiangxi Province provide chronostratigraphic constraints on the Shanghuan–Nongshanian Asian Land Mammal Age boundary and allow for a more accurate determination of an early Paleogene paleomagnetic pole for the South China Block. Paleomagnetic analysis of 121 sites (326 samples) reveals that the Shanghuan–Nongshanian boundary lies close to a normal-to-reverse polarity change. Stable carbon isotope analysis of dispersed organic matter and paleosol carbonates indicate a secular increase of ~1.5‰ superimposed on higher frequency variations. Correlation of this magnetochemostratigraphic pattern to the global timescale suggests that the polarity reversal near the Shanghuan–Nongshanian boundary likely represents the Chron C27n–C26r transition. The Torrejonian–Tiffanian North American Land Mammal Age boundary is closely correlated to this same polarity transition, indicating nearly synchronous global mammalian turnover at this time. Because both Land Mammal Age boundaries are thought to record turnover of mostly endemic taxa, it is unlikely that the synchroneity of faunal change is due to intercontinental dispersal as documented for other early Paleogene faunal transitions (e.g. Paleocene–Eocene boundary). Instead, these mammalian faunal transitions may represent independent ecological or evolutionary responses to environmental changes that have been interpreted from marine records at this time (e.g. "Top Chron 27n Event"). These new paleomagnetic results from the Chijiang Basin are also used to augment other published data and to calculate a Paleocene paleomagnetic pole for the South China Block. The new pole shows no significant vertical axis rotation compared to the Paleocene reference pole for Eurasia indicating that much of the clockwise rotation that has been documented for the South China Block from Cretaceous deposits cannot be the result of extrusion tectonics associated with the early Paleogene India–Asia collision. Observed Cretaceous rotations of the South China Block may be the result of late Cretaceous–early Paleocene rifting in the backarc of the Kula–Pacific subduction zone.

1. Introduction

Land Mammal Age (LMA) frameworks are biochronological systems developed for terrestrial sediments that identify periods of major intra-continental mammalian turnover. Recent progress in correlating these independent continental biostratigraphic frameworks to the global timescale (and thus to each other) has established the intercontinental synchroneity for several major mammalian turnover events (Woodburne and Swisher, 1995). For example, the Paleocene–Eocene boundary is marked by rapid global warming and coincident dispersal-related mammalian turnover in the holarctic continents (Gingerich, 1989; Koch et al., 1992; Clyde and Gingerich, 1998; Bowen et al., 2002; Gingerich, 2003). The mammalian turnover at the Paleocene–Eocene boundary defines the Clarkforkian–Wasatchian LMA boundary in North America, the Gashatan–Bumbanian LMA boundary in Asia, and the Cernaysian–Neustrian LMA boundary in Europe (Gingerich, 1989; Hooker, 1998; Beard, 1998). Many of the Land Mammal Age boundaries, such as those during the Paleocene of Asia, remain poorly correlated to the time scale, making it difficult to determine the ubiquity of such synchronized intercontinental turnover. The Paleocene Asian Land Mammal Ages (ALMA) are best documented from fossiliferous syntectonic deposits in the rift basins of south China that formed due to extension in the backarc of the Kula–

* Corresponding author. Tel.: +1 603 862 3148; fax: +1 603 862 2649.
E-mail address: will.clyde@unh.edu (W.C. Clyde).

0012-821X/$ – see front matter © 2008 Elsevier B.V. All rights reserved.
doi:10.1016/j.epsl.2008.03.009

Pacific subduction complex during the late Cretaceous and early Tertiary (Ren et al., 2002). Active subsidence associated with these extensional structures created considerable accommodation space for the accumulation of clastic detritus eroded from nearby uplands. Here we present new paleomagnetic, biostratigraphic, and chemostratigraphic information from a ~1000 meter thick Paleocene sedimentary sequence in the Chijiang Basin of Jiangxi Province in an effort to better constrain the timing of the Shanghuan–Nongshanian ALMA boundary.

The paleomagnetic data presented here are also used to evaluate the far-field tectonic impact of the India–Asia collision. The Chijiang Basin is located on the South China Block, which is one of several tectonic blocks that have sutured together to form the Asian continent (Fig. 1). Although these blocks are thought to have been sutured together during the Mesozoic or before (Zhang et al., 1984), there is considerable interest in testing whether they underwent appreciable post-accretion rotation during the Cenozoic (Kent et al., 1986; Enkin et al., 1992; Huang and Opdyke, 1992; Gilder et al., 1993; Zhao et al., 1994, Morinaga and Liu, 2004; Sun et al., 2006; Huang et al., 2007; Wang and Yang, 2007). For instance, one hypothesis, the 'extrusion' hypothesis, suggests that as much as 1000 km of sinistral motion occurred along the Red River Fault separating Indochina from South China in order to accommodate the large magnitude of crustal shortening that occurred during the India–Asia collision (Molnar and Tapponnier, 1975; Tapponier et al., 1982; Sato et al., 2001). Other studies point to extrusion along faults further to the north (e.g. Mongol–Okhotsk suture; Halim et al., 1998) or to changes in the relative motion between the Asian and Pacific plates as key factors in the late Cretaceous and Tertiary tectonics of China (Taylor and Hayes, 1983; Xu et al., 1987). In order to understand the post-accretion mobility of these major continental blocks, there is a need for better resolved paleomagnetic data from the early Cenozoic deposits of these blocks (Zhao et al., 1994). Our results from Chijiang Basin bolster the existing database of early Paleogene paleomagnetic information for the South China Block and allow further evaluation of both intra- and inter-block rotations for this part of Asia.

2. Geological setting

The Chijiang Basin is an elongate graben on the northern flank of the Nanling Mountains in southern Jiangxi Province. The Paleogene red beds in Chijiang Basin have been divided into 3 formations (Shizikou Formation, Chijiang Formation, and Pinghu Formation from bottom to top) that are similar lithologically and thus difficult to distinguish in the field (Zheng et al., 1973; Tong et al., 1976, 1979). The Shizikou Formation is characterized by homogenous red mudstones without obvious bedding features except for a few thin conglomeratic beds. The overlying Chijiang Formation is also red in color but is lithologically more heterogenous (mudstones, laminated siltstones, channel sandstones) and, in places, preserves evidence of pedogenesis and bioturbation. The Chijiang Formation is divided into two members, the lower Lannikeng Member and the upper Wangwu Member (Tong et al., 1976). The Pinghu Formation overlies the Chijiang Formation and is characterized by repetitive packages of laminated yellowish grey clay (~1 m thick) interbedded with unlaminated red mudstones (~2.5 m thick). The best exposure of Pinghu Formation lies in the northeastern part of the basin where its depositional relationship to the other units is not well constrained due to intervening overburden. The lithological variations in these stratigraphic units indicate that the Chijiang Basin was characterized by a rapidly accumulating, highly oxidizing, fluvio-lacustrine depositional system during the Paleocene.

Field parties from the Institute of Vertebrate Paleontology and Paleoanthropology (IVPP) began prospecting for fossils in the Chijiang Basin in the 1970s and at present there are 21 known fossil localities, although some of these localities have been destroyed in recent years due to agricultural development in the area (Li and Ting, 1983; Russell and Zhai, 1987). Several important fossils are known from this basin, and it is the only basin currently known in Asia that preserves a relatively continuously exposed Shanghuan–Nongshanian ALMA boundary (Tong et al., 1976, 1979; Tong, 1979a,b,c; Tong and Huang, 1986; Ting et al., 2007).

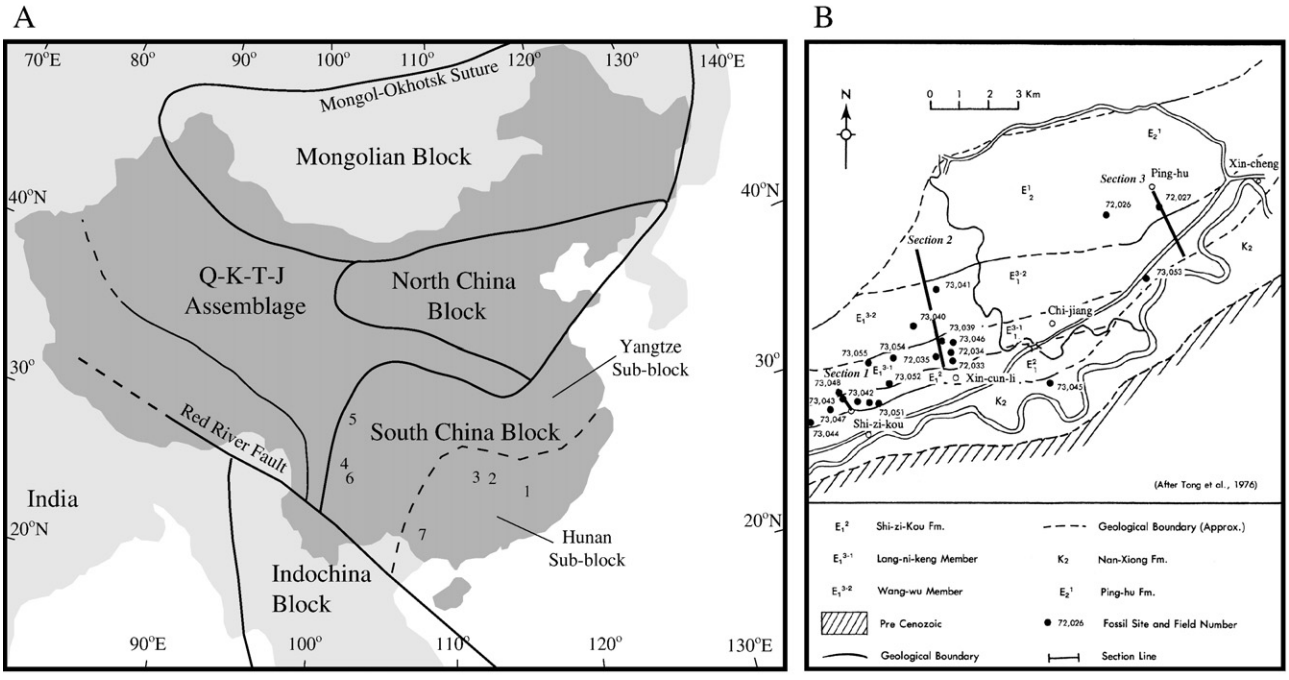

Fig. 1. (A) Map of China showing major tectonic blocks that make up the eastern part of Asia. Heavy lines mark boundaries between major blocks and dashed lines mark boundaries between secondary blocks. Numbers on map represent approximate locations of studies discussed in this paper and correspond to the numbers in Table 1. Q–K–T–J assemblage is Qaidam–Kunlun–Tarim–Junggar terranes. Map is modified from Enkin et al. (1991) and Hsu et al. (1988). (B) Map modified from Tong et al. (1976) showing the Chijiang Basin geology, position of fossil localities, and the location of the three stratigraphic sections discussed in this paper.

3. Paleocene Asian Land Mammal Ages

There are three Paleocene ALMAs (Shanghuan, Nongshanian, and Gashatan) and the boundaries between them represent significant reorganizations of Asian mammalian faunas. The Shanghuan is the oldest and was established largely based on work in the Nanxiong Basin, Guangdong province, China. It was first presented as a tentative "Chinese Provincial Age" that correlated to the Puercan and Torrejonian North American Land Mammal Ages (NALMA; Li and Ting, 1983; Tong et al., 1995). Later the Shanghuan was correlated to the Puercan through the mid-Torrejonian NALMA (Pu-To2) by Wang et al. (1998), and to the Torrejonian NALMA by Ting (1998). The Shanghuan was most recently defined to include the time between the first appearance of the order Pantodonta, represented by *Bemalambda*, and the first appearance of the order Arctostylopida, represented by *Asiostylops* (Ting, 1998). Several mammalian orders, including Anagalida, Acreodi, Tillodontia, and Condylarthra, and families, including Didymoconidae, Eurymylidae, and Mimotonidae, also made their first appearance during this interval. The Shanghuan is characterized by a prevalence of Asian endemic forms.

The Nongshanian ALMA was established mainly based on work in the Nanxiong Basin and the Chijiang Basin. The Nongshanian was first proposed as a tentative late Paleocene "Chinese Provincial Age" and correlated to the Tiffanian NALMA (Li and Ting, 1983). It was later correlated to the Tiffanian through Clarkforkian NALMA (Tong et al., 1995), to the Tiffanian NALMA (Ting, 1998), or to the late Torrejonian through late middle Tiffanian NALMA (To3–Ti4; Wang et al., 1998). It has traditionally been defined as the time between the first appearance of the order Arctostylopida, represented by *Asiostylops*, and the first appearance of the order Rodentia, represented by *Tribosphenomys* (Ting, 1998). The family Phenacolophidaea and Ernanodontidae also made their first appearance in the interval and several species of *Archaeolambda* are very common during this interval. The Nongshanian is characterized by the reduction of Asian endemic forms and appearance of taxa closely related to Rodentia (e.g. *Heomys orientalis*), Lagomorpha (e.g. *Mimotona wana*), and Perissodactyla (e.g. *Radinskya yupingae*).

The Gashatan was first proposed by Romer (1966) to represent a late Paleocene ALMA based on work in the Nemegt Basin, Mongolia. It was later defined by Szalay and McKenna (1971) as "the joint overlapping time ranges of *Palaeostylops, Pseudictops, Prionessus*, and *Eurymylus*" and inferred to be "latest Paleocene in age". The Gashatan was most recently defined to include the time between the first appearance of the order Rodentia, represented by *Tribosphenomys*, and the first appearance of the order Perissodactyla, represented by *Orientolophus* (Ting, 1998). The order Multituberculata and pantodont family Coryphodontidae also made their first appearance during this interval. The Gashatan has been variously correlated to the Tiffanian NALMA (Romer, 1966), the Clarkforkian NALMA (Ting, 1998) and the late Tiffanian through Clarkforkian NALMA (Wang et al., 1998). The Gashatan is characterized by the further reduction of Asian endemic forms and the increased shared occurrence of taxa with North America (e.g. *Coryphodon*).

4. Methods

We sampled a total of 121 sites for paleomagnetic and isotopic analysis from three stratigraphic sections within the Shizikou, Chijiang, and Pinghu Formations in the southwestern part of Chijiang Basin. The Paleogene strata in the Chijiang Basin are gently tilted with dips shallowing toward the northwest. Section 1 (230 m thick, 22 sites) begins near the village of Shizikou within the Shizikou Formation and ends in the lower Chijiang Formation near the village of Tianxinli. Section 2 (730 m thick, 82 sites) lies entirely within the Chijiang Formation and begins near the village of Xincunli and ends near the village of Wang Wu. Exposure of these sections is relatively good and trigonometric projection indicates that the top of Section 1 correlates closely with the base of Section 2. Section 3 (265 m thick, 19 sites), which lies farther to the east, is not well exposed and is difficult to correlate to the other sections due intervening overburden. Given these uncertainties, we do not interpret the magnetostratigraphy from Section 3 but do include the samples from this part of the basin for purposes of applying the fold test and to increase the precision of our paleomagnetic pole.

Paleomagnetic samples were taken as oriented hand samples, and later cut into ~2.5 cm cubes, or were drilled as oriented 1-inch diameter cores. All analyses were conducted in the paleomagnetics laboratory at University of New Hampshire using an HSM2 SQUID cryogenic magnetometer, Molspin tumbling AF demagnetizer, and an ASC Model TD48-SC thermal demagnetizer. Remanence components were determined by least-squares analysis and site statistics were determined using the methods of Fisher (1953). Virtual Geomagnetic Pole (VGP) positions were calculated for each site and these were averaged to calculate a mean paleomagnetic pole for the entire study. Stratigraphic sections were measured using Jacob staff and abney level. GPS location and stratigraphic level were determined for each sample site.

Sediment samples (cm- to dm-sized blocks) for total organic carbon concentration (TOC) and bulk $\delta^{13}C$ analysis were collected from freshly exposed rock surfaces at the same stratigraphically-keyed localities where paleomagnetic samples were taken. The geochemical samples were prepared and analyzed at the University of California, Santa Cruz Stable Isotope Lab. Surficial material was removed from sample blocks and ~2 g interior pieces were powdered with a mortar and pestle. All powders were then acidified using 10% HCL, rinsed with milliQ water until the solution had a neutral pH, and dried at 60 °C overnight, or until visibly dry. Samples were repowdered with a mortar and pestle and further cleaned with dicloromethane (DCM) to remove soluble organics and left overnight to volatilize. Processed samples were analyzed on a Carlo-Erba CHN-O Elemental Analyzer (EA) coupled to a ThermoFinnegan DeltaPlus XP continuous flow mass spectrometer. Samples were initially analyzed to determine weight percent carbon; subsequent carbon isotope analysis was done with samples grouped by weight %. All carbon isotope values are reported in delta notation relative to the V-PDB standard: $\delta = [(R_{sample}/R_{V\text{-}PDB}) - 1] \times 1000$, where R_{sample} and $R_{V\text{-}PDB}$ are the isotope ratios of the sample and standard, respectively. Analytical precision for $\delta^{13}C$ values and TOC concentrations (in wt.% carbon) is based on two in-house standards, Acetanilide and PUgel. Standard deviation for Acetanilide $\delta^{13}C$ values was 0.87‰ and 7.21% for TOC concentration ($n=92$). Standard deviation for PUgel $\delta^{13}C$ values was 0.28‰ and 4.02% for TOC concentrations ($n=112$). PUgel precision was better than Acetanilide precision, and this is likely due to difficulty in weighing small amounts of Acetanilide. For both standards, error in the TOC concentration is ~10% of the overall proportion of carbon in the sample.

Pedogenic carbonate nodules were sampled when possible although they were relatively rare in Chijiang Basin facies. Nodules were polished flat on a lapidary wheel, washed, and then dried at 60 °C. Primary micritic carbonate (~100 μg) was drilled from the polished surface under a binocular microscope using a mounted dental drill. Samples were roasted in vacuo at 400 °C for 1 hour to remove organic contaminants and analyzed with a gas source mass spectrometer following reaction with 100% phosphoric acid at 90 °C using an Isocarb device. Samples were analyzed using either the Optima or the Prism mass spectrometer in the Departments of Earth and Ocean Sciences, University of California, Santa Cruz. Carbon isotope values are reported in delta notation relative to the V-PDB standard. Analytical precision, based on the standard deviation for repeated analysis of an in-house standard, was <0.07‰.

5. Results

5.1. Biostratigraphy

Several fossil localities are correlated to the stratigraphic sections presented here. Localities in the lower half of Section 1 (Shizikou

Formation) contain the pantodont *Bemalambda* which is typical of the Shanghuan Land Mammal Age. Localities from the upper part of Section 1 and the majority of Section 2 are characterized by Nongshanian land mammals such as *Harpyodus decorus*, *Asiostylops spanios* (in the Lannikeng member of the Chijiang Fm.), and *Bothriostylops notios* (in the Wangwu member of the Chijiang Fm.). The Shanghuan–Nongshanian boundary is reasonably well constrained to fall between 73 and 121 m in Section 1. This 50 meter uncertainty likely represents <200 kyr in this rapid accumulation environment. A single locality at the top of Section 3 contains the primitive uintathere *Prodinoceras*, which is typical of the Gashatan ALMA. Unfortunately, the relationship of this fossil locality to the stratigraphic framework reported here is too uncertain to confidently constrain the age of the Nongshanian–Gashatan ALMA boundary.

5.2. Paleomagnetism

During thermal demagnetization, most paleomagnetic samples showed stable demagnetization behavior with 1–2 components of magnetization (Fig. 2). Many specimens carried a low temperature component (typical unblocking temperatures <350 °C) that exhibits directions consistent with a present-day field overprint. Most specimens exhibited a strong high-temperature characteristic component that unblocked near 690 °C indicating a hematite carrier. The characteristic high-temperature components were used to calculate site statistics and these were then used to construct a magnetostratigraphy and calculate an average paleomagnetic pole for the early Paleogene of the Chijiang Basin.

Sites were coded according to their reliability. Alpha sites ($n=73$) were those that have 3 or more stable samples that are significantly clustered at $p \le 0.05$ (Table DR1; Watson, 1956). Beta sites ($n=7$) were those that have 3 stable samples significantly clustered at $p \le 0.05$ but where one sample was characterized by a great circle direction. Alpha sites exhibit antipodal directions in tilt adjusted coordinates with an average declination/inclination of 12.8°/23.5° ($\alpha_{95}=4.0°$) when all reversed sites are inverted (Fig. 2). This characteristic component passes the reversal test at the 95% confidence limit using the bootstrapping method (Tauxe, 1998; Figure DR1). The alpha sites also pass the bootstrap fold test despite relatively little difference in bedding orientations, showing maximum clustering near 100% unfolding and a 95% confidence interval that excludes 0% unfolding (Tauxe, 1998; Figure DR2). Beta sites are used here for purposes of magnetostratigraphy but are not included in the calculation of a paleomagnetic pole due to their lower reliability.

When these paleomagnetic data are plotted against stratigraphic level, Section 1 has two main polarity zones (A+ and B−; Fig. 3). Section 2 is characterized by a single long zone of reversed polarity that is inferred to be the same as zone B− of Section 1 given the projected overlap of the top of Section 1 with the base of Section 2. From this intrabasinal correlation we have created a composite polarity record that can be correlated to the GPTS (Fig. 3).

5.3. TOC and stable isotopes

TOC concentrations and $\delta^{13}C$ values of bulk organic carbon ($\delta^{13}C_{org}$) were significantly different for the 3 local sections (ANOVA, $p \ll 0.001$; Tables DR2–3). For Section 2, which had the longest and

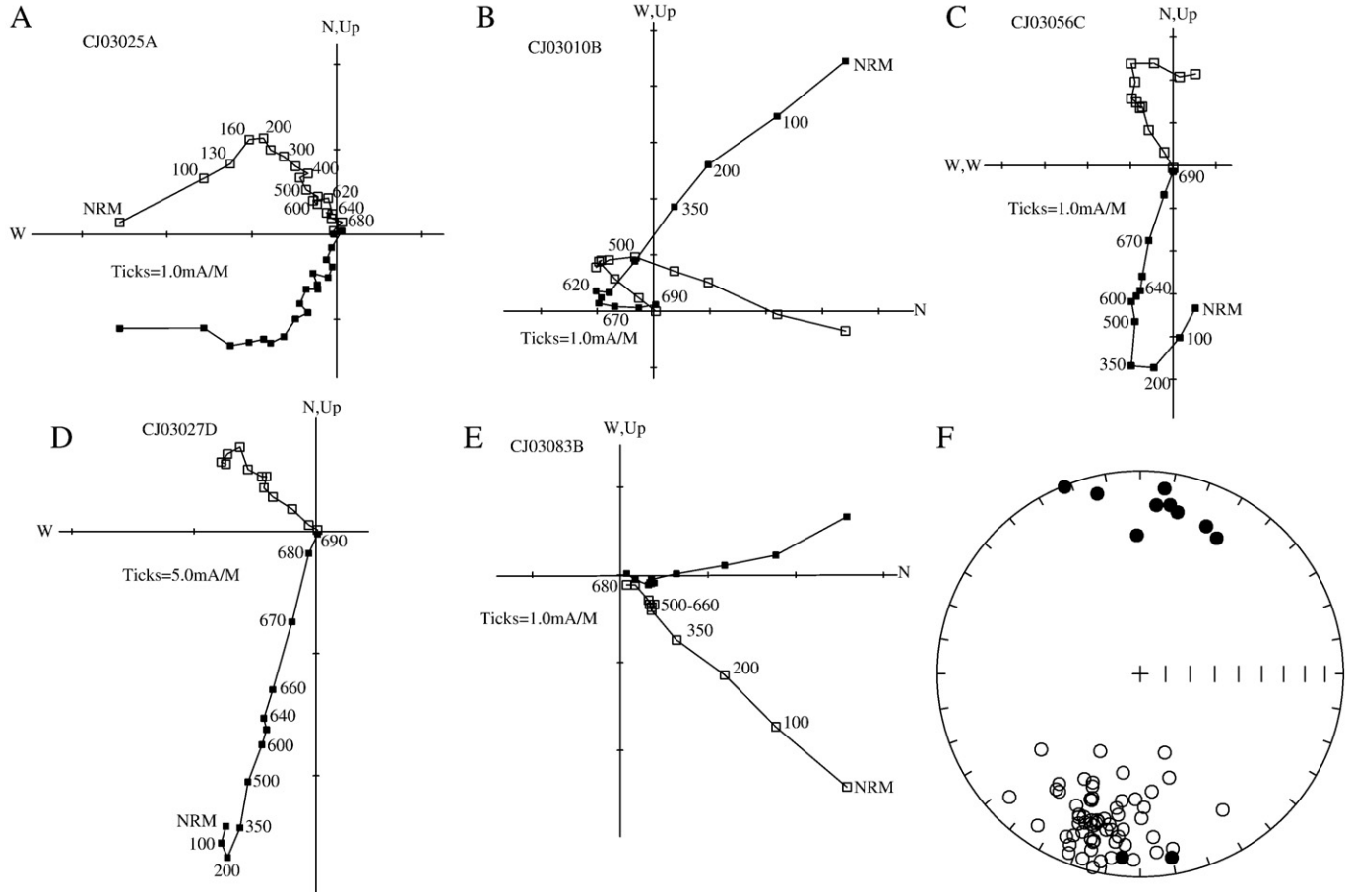

Fig. 2. (A–E) Representative vector endpoint diagrams of paleomagnetic samples analyzed from the Chijiang Formation (A–D) and the Shizikou Formation (E) of the Chijiang Basin. Open (closed) symbols show vector endpoints in the vertical (horizontal) plane. (F) Equal area projection of mean site directions for alpha sites from the Chijiang Basin. Open (closed) symbols lie on the upper (lower) hemisphere of the projection. All directions are shown in tectonically corrected coordinates.

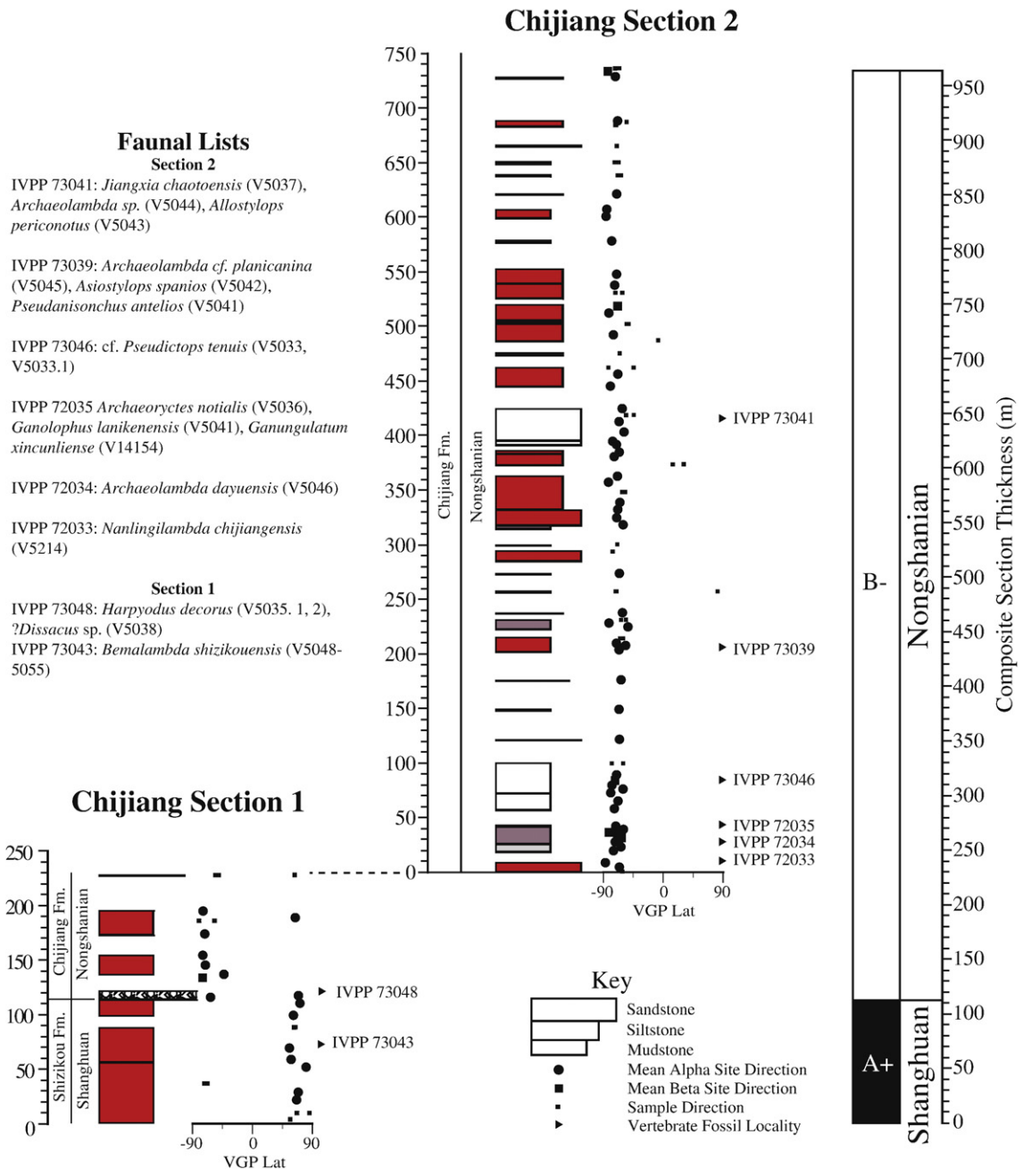

Fig. 3. Stratigraphy of Sections 1 and 2 from Chijiang Basin. Lithology is shown for the intervals of section that are exposed and VGP latitude for alpha (large circles), beta sites (large squares), and samples from other sites (small squares) are plotted against stratigraphic level (meters). Sections are aligned according to correlations made in the field and trigonometric projection. Width of lithological beds represents grain size as shown in key whereas the shading represents color. Vertebrate fossil localities and stratigraphic position of key fossil localities are listed to right of lithological sections. Faunal lists for localities are given in top left of figure.

highest fidelity record (see below), we replicated analyses of most organic carbon samples between two and seven times. Between-replicate $\delta^{13}C$ value differences averaged 1.1‰, with a standard deviation of 1.5‰. We culled replicates with differences greater than 2.6‰ (the sum of the average difference and one standard deviation) if the replicate was responsible for the majority of difference in the sample. This resulted in discarding 21 "outlier" samples out of a total of 225 replicate samples that were analyzed. Section 2 sample averages were calculated based on the culled data set (Table DR2). Before culling, replicate differences in TOC concentrations averaged 0.008% with a standard deviation of 0.015%. We used TOC concentration indirectly in the culling process as an additional monitor of replicate irregularity.

TOC concentrations for Section 2 were an order of magnitude lower (mean=0.05% at Section 2 vs. 0.95% and 0.56% at Sections 1 and 3) and less variable (1σ=0.07% vs. 0.35 and 0.36%) than at either of the other sections (Tables DR2–3). The $\delta^{13}C_{org}$ at Section 2 are much lower than those at the other 2 sections (mean=−22.1‰ vs. −9.9‰ and −11.5‰). The measured TOC concentrations and isotopic compositions for Section 2 samples are similar to those observed in other Paleocene paleosols and redbeds and are consistent with the expected range of values for organic carbon derived from a Paleocene C3 ecosystem (e.g., Koch et al., 2003). In contrast, the $\delta^{13}C_{org}$ values at Sections 1 and 3 indicate carbon originating primarily from C4 plants (O'Leary, 1995), which are not known from the early Paleogene (e.g., Arens et al., 2000) but are common within the modern flora of southeast Asia (Still

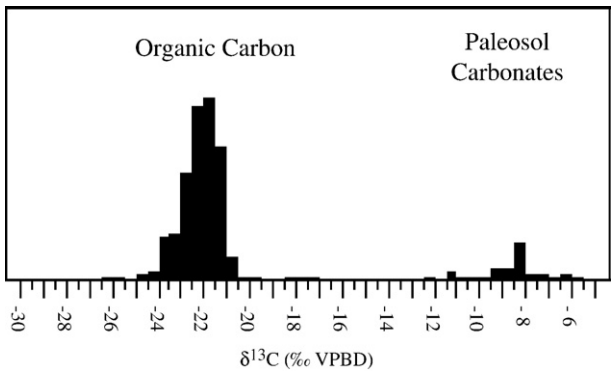

Fig. 4. Histogram of $\delta^{13}C$ values of organic carbon and paleosol carbonates from Chijiang Formation of Section 2. The low values of organic carbon and the ~15‰ difference between organic carbon and carbonate values is consistent with the expected values of a Paleocene C3 ecosystem.

et al., 2003). The association of high $\delta^{13}C_{org}$ values with high TOC concentrations and the lack of any offset between $\delta^{13}C_{org}$ and the $\delta^{13}C$ of paleosol carbonate ($\delta^{13}C_{carb}$) for Sections 1 and 3 indicate strongly that the organic samples from these two sections were contaminated with modern organic carbon (See discussion in Data repository and Tables DR3 and 5).

In contrast to Sections 1 and 3, Section 2 seems to have preserved a reliable record of Paleocene soil organic matter. This interpretation is supported by the observation that Section 2 samples have low TOC contents and, unlike the other sections, exhibit no correlation between TOC and $\delta^{13}C_{org}$ values (Tables DR2 and 4). In addition, Section 2 samples show the expected ~15‰ offset between $\delta^{13}C_{carb}$ and $\delta^{13}C_{org}$ (Fig. 4). The $\delta^{13}C_{org}$ results from Section 2 show high frequency variability superimposed on a secular increase in mean values of ~1.5‰ going up section (Fig. 5; Table DR2). The $\delta^{13}C_{carb}$ results show much the same pattern (aside from one very low outlier at ~400 m) however sample resolution is lower than the $\delta^{13}C_{org}$ results due to the relative rarity of paleosol carbonates in these facies (Table DR4; Figure DR5).

6. Discussion

6.1. Magnetochemostratigraphy

The pattern of magnetic polarity reversals in the Chijiang sections can be used to correlate to the Geomagnetic Polarity Time Scale (GPTS, Gradstein et al., 2004). Constraints on the correlation include the K/T boundary below the base of our section, previously published pilot paleomagnetic results from the nearby Nanxiong Basin indicating that the Shanghuan ALMA extends stratigraphically above C28n (Zhao et al., 1991), the long reversed polarity zone that makes up the majority of our composite section, and the overall ~1.5‰ increase in average $\delta^{13}C$ of organic matter. These constraints favor the correlation of the normal (zone A+) to reverse (zone B−) polarity transition near the base of our composite section to the Chron C27n to C26r reversal (Fig. 5). This correlation is favored because Chron C26r is quite long (in fact, it is the longest interval of reversed polarity for the entire Cenozoic), which matches the long polarity zone B−, and corresponds to a secular increase of ~1.5‰ in the marine $\delta^{13}C$ composite record (Zachos et al., 2001), which matches the observed local increase in $\delta^{13}C$. Although the observed variability in $\delta^{13}C_{org}$ in Section 2 could reflect local paleoenvironmental changes (e.g. aridity, floral composition, or physiography), the relative homogeneity of sedimentary facies (and by inference depositional environments) throughout Section 2 supports the interpretation that the increase in mean values tracks the global change in the carbon isotope budget.

Although the combination of the long duration and increasing carbon isotopic trend of Chron C26r is unique for the Paleocene,

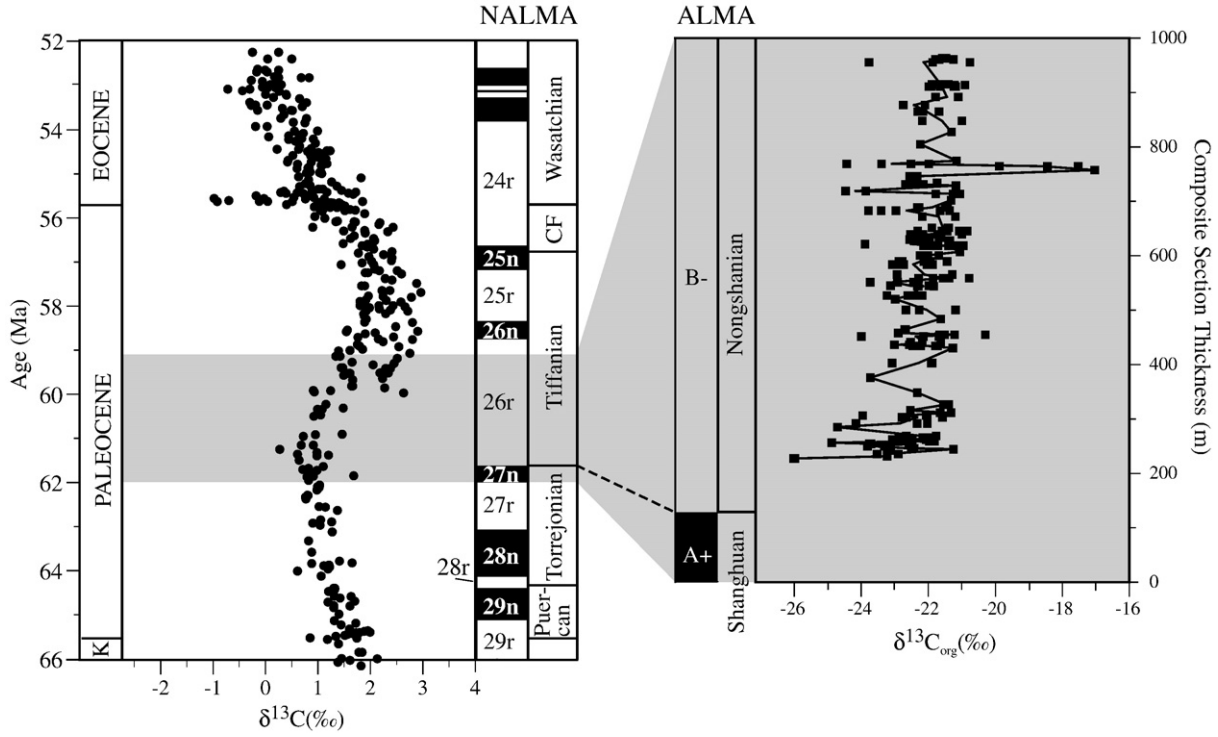

Fig. 5. (Right) Carbon isotope values of organic carbon samples from Chijiang Section 2 correlated to the composite magnetobiostratigraphy from Fig. 3. (Left) Preferred correlation of the Chijiang Basin record to the North American Land Mammal Age framework (Lofgren et al., 2004), GPTS (Gradstein et al., 2004), and composite $\delta^{13}C$ record of benthic foraminifera from the deep sea (Zachos et al., 2001; ages recalibrated to Gradstein et al., 2004). This preferred correlation suggests that the Shanghuan–Nongshanian ALMA boundary is nearly coincident with the Torrejonian–Tiffanian NALMA boundary. It is also possible that the A+ polarity zone in the Chijiang composite section represents Chron C28n or even C29n with the intervening time missing due to an unconformity (see text for discussion).

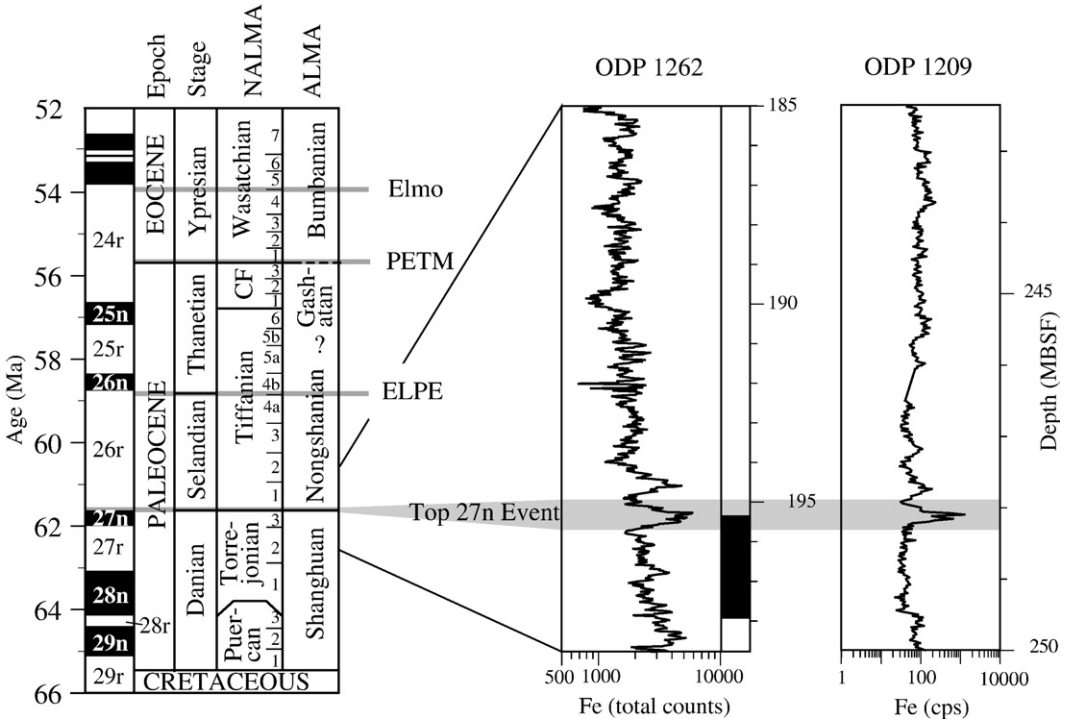

Fig. 6. Summary chronostratigraphy for the Paleocene and early Eocene (left) showing preferred correlation of marine stages, North American Land Mammal Ages (NALMAs), and Asian Land Mammal Ages (ALMAs). Stratigraphic record of iron concentration from ODP sites 1262 and 1209 (right) showing peaks that define the "top Chron C27n event" of Westerhold et al. (2007). Putative "hyperthermal" events that have been identified from the literature are shown with light grey shading (Elmo, PETM, ELPE, Top 27n event; Lourens et al., 2005; Westerhold et al., 2007). Notice the coincidence of significant marine and continental biotic turnover, in the form of biostratigraphic boundaries, with the hyperthermal events. Figure is adapted from Gradstein et al. (2004), Lofgren et al. (2004), Clyde et al. (2007), Bowen et al. (2002), Bowen et al. (2005), and Westerhold et al. (2007).

making it very probable that zone B− corresponds to Chron C26r, the correlation of zone A+ to Chron C27n is less certain. The observed polarity reversal between zones A+ and B− occurs at a conglomeratic channel deposit, the base of which likely represents an unconformity, so it is possible that zone A+ is Chron C28n or even C29n with the intervening time missing due to the unconformity. We consider the existence of such a major unconformity here to be unlikely as channel deposits of this scale are common features in fluvio-deltaic depositional environments and the small extensional basins of southeast China were characterized by relatively continuous sedimentation during this period (Ren et al., 2002). In addition, preliminary paleomagnetic results from the nearby Nanxiong Basin (Zhao et al., 1991) suggest that the Shanghuan ALMA extends up into Chron C27r which, when combined with the evidence presented here showing that the Nongshanian extends down to Chron C26r, indicates that the Shanghuan–Nongshanian ALMA boundary almost certainly lies somewhere in the ~0.7 myr between the upper part of Chron C27r and the lower part of Chron C26r. Given these various constraints and uncertainties, we prefer the parsimonious interpretation that the zone A+ to B− polarity transition that marks the Shanghuan–Nongshanian ALMA boundary in the Chijiang Basin represents the Chron C27n–C26r reversal but acknowledge the need to further test this correlation. Assuming our preferred correlation is correct, the new stratigraphic framework indicates that the Shanghuan–Nongshanian ALMA boundary correlates closely to the Torrejonian–Tiffanian NALMA boundary as that boundary is also known to occur near the top of Chron C27n (Butler et al., 1987; Lofgren et al., 2004). This result adds to increasing evidence for coincident turnover in land mammal faunas on holarctic continents during the Paleogene. For instance, there is clear evidence for rapid mammalian dispersals at the Paleocene–Eocene boundary coincident with the short but intense interval of global warming known as the Paleocene–Eocene Thermal Maximum (PETM; Clyde and Gingerich, 1998; Bowen et al., 2002; Gingerich, 2003). The potential coincidence of the Shanghuan–Nongshanian ALMA boundary and the Torrejonian–Tiffanian NALMA boundary is different from the turnover at the Paleocene–Eocene boundary as it is not thought to be associated with a major intercontinental dispersal event. The turnover events that define the Shanghuan–Nongshanian ALMA boundary and the Torrejonian–Tiffanian NALMA boundary are dominantly among mammal groups that are endemic to their respective continents (Archibald et al., 1987), and the Torrejonian–Tiffanian boundary is less abrupt than would be expected for a PETM like dispersal event (Higgins, 2003). In addition, there are no shared genera in the mammal faunas from these continents at this time. In the absence of evidence for intercontinental dispersal, the inferred coincidence of these mammalian turnovers may indicate independent biotic responses to a common underlying environmental perturbation.

Holarctic mammalian turnover is not the only evidence for significant biotic and environmental changes near the top of Chron C27n. For instance, the Danian–Selandian Stage boundary (early–middle Paleocene) has traditionally been defined in marine sections at the P2–P3 planktic foraminiferal zone boundary, which occurs at the top of Chron C27n and thus also likely correlates with the land mammal age boundaries discussed here (Berggren et al., 1995; Gradstein et al., 2004).[1] Furthermore, detailed cyclostratigraphic records from ODP Leg 208 on Walvis Ridge (South Atlantic) and ODP site 1209 from Shatsky Rise (Western Pacific) indicate high peaks in iron concentration at the top of Chron C27n referred to as the "Top Chron C27n Event" (Westerhold et al., 2007; Fig. 6). Other such peaks in iron content (and correlated magnetic susceptibility) in Walvis Ridge cores record dissolution at hyperthermal events like ELPE[2], PETM, and Elmo

[1] Recently, the Paleocene Working Group has proposed a new GSSP for the Danian-Selandian Stage boundary that lies stratigraphically above the top of Chron C27n however it has not yet been formally approved [International Subcomission on Paleogene Stratigraphy; http://wzar.unizar.es/isps/wgr.htm].

[2] The ELPE ("Early-Late Paleocene Event") event of Westerhold et al. (2007) is equivalent to the MPBE ("Mid-Paleocene Biotic Event") of Bralower et al. (2006), Zachos et al. (2004), and Bernaola et al. (2007).

Table 1
Summary of paleomagnetic information for Paleocene/Eocene sites on the South China Block

Basin/Province	ϕ_p	λ_p	A95	*N* (sites)	Lat	Lon	Ref	Formation	Age	Sub-block
1. Chijiang Basin/Jiangxi	248.3	72.4	3.5	73	25.5	114.5	This study	Chijiang Formation	Paleocene	Hunan
2. Hengyang Basin/ Hunan	300.7	82.6	4.4	22	26.9	112.6	Sun et al. (2006)	Dontang&Xialiushi	Paleocene	Hunan
3. Hengyang Basin/Hunan	256.4	73.6	5.6	19	27	112	Bowen et al. (2002)	Lingcha Formation	Paleocene/Eocene	Hunan
4. Huili area/ Sichuan	286.1	70.6	11.6	7	26.4	102.3	Huang and Opdyke (1992)	Leidashu	Pal–Eoc	Yangtze
5. Sichuan Basin/Sichuan	299.9	76.8	3.6	7	30	103	Enkin et al. (1991)	Jin Gi Guan, Yu Guang Po, Lu Shan	Paleocene	Yangtze
6. Lunan and Kunming Basins/Yunnan	325.2	84.4	7.6	2	24.5	103	Qizhong et al. (1986)	Lumeiyi and Xiaotun Formations	Eocene–Oligocene	Yangtze
7. Nanning Basin/Guangxi	236	83.8	4.3	5	22.8	108.4	Zhao et al. (1994)	Fenghuangshan	M. Eocene	Hunan
				N (poles)						
Hunan Sub-block (poles 1–3, 7)	257.1	78.8	8.5	4						
Yangtze Sub-block (poles 4–6)	296.5	77.6	11.9	3						
South China Block (poles 1–7)	274.9	78.9	6.1	7						

ϕ_p, λ_p are longitude and latitude of the paleomagnetic pole from the study; A95 is circle of 95% confidence; *N* is number of sites (above) or poles (below) used in calculating the average; Lat and Lon are the latitude and longitude of the study site in decimal degrees; Ref is the literature reference which was used to obtain the data; Formation is the geological unit that was sampled; Age is the age range of the samples from that study; Sub-block is the terrane on the South China Block from which the samples are derived.

(Lourens et al., 2005; Westerhold et al., 2007), however so far there is no clear isotopic evidence for a hyperthermal at the Top Chron 27n Event (e.g. Quillevere et al., 2002). Whatever their cause, these deep sea dissolution events seem to correspond to known turnovers in land mammal assemblages in North America and possibly Asia (Fig. 6). Taken together, these observations suggest the possibility of global environmental change near the top of Chron C27n that affected both continental and marine systems.

6.2. Tectonics

The 'extrusion' model of Asian deformation suggests that some of the post-collision shortening between India and Asia was accommodated by the translation and rotation of major Asian tectonic blocks. Although there is clear evidence for >30° of clockwise rotation of the Indochina block along the Red River fault in response to India–Asia collision (Sato et al., 2001, 2007), evidence for significant rotations of (or within) the other major Asian blocks like the South China Block (SCB) is less clear. Most paleomagnetic studies that have sampled the SCB to test the extrusion model have focused on Cretaceous sediments (however see Zhao et al., 1994) and the results have been mixed, with some studies showing significant intra and/or inter-block clockwise rotations and others not (Kent et al., 1986; Enkin et al., 1991, 1992; Gilder et al., 1993; Morinaga and Liu, 2004; Sun et al., 2006; Huang et al., 2007; Wang and Yang, 2007). Because the initial India–Asia collision did not occur until the late Paleocene or later (Patriat and Achache, 1984; Beck et al., 1995; Rowley, 1996; Clyde et al., 2003; Aitchison et al., 2007), these Cretaceous studies significantly predate the collision and thus may incorporate rotations associated with other tectonic processes occurring after the depositional age of the rock but before the age of India–Asia collision. This window of potential tectonic 'underprinting' is quite long (>10 myr) and includes some well-documented regional tectonic events such as the backarc extensional effects of the nearby Kula–Pacific subduction zone (Ren et al., 2002). With increasing numbers of studies being carried out on early Paleogene rocks of the SCB like those studied here, it is now possible to eliminate the effects of these older tectonic processes and test more precisely for extrusion-related rotations.

The new paleomagnetic data reported here from the Chijiang Basin were used to calculate a paleomagnetic pole for this study site, which was then compared to other early Paleogene poles from the South China Block and to poles for other Asian blocks and 'stable' Eurasia (Tables 1 and DR1). The Chijiang pole (Φ_p=248.3, λ_p=72.4, α_{95}=3.5) is in good agreement with other early Paleogene poles calculated for stable parts of the South China Block. Published paleomagnetic poles

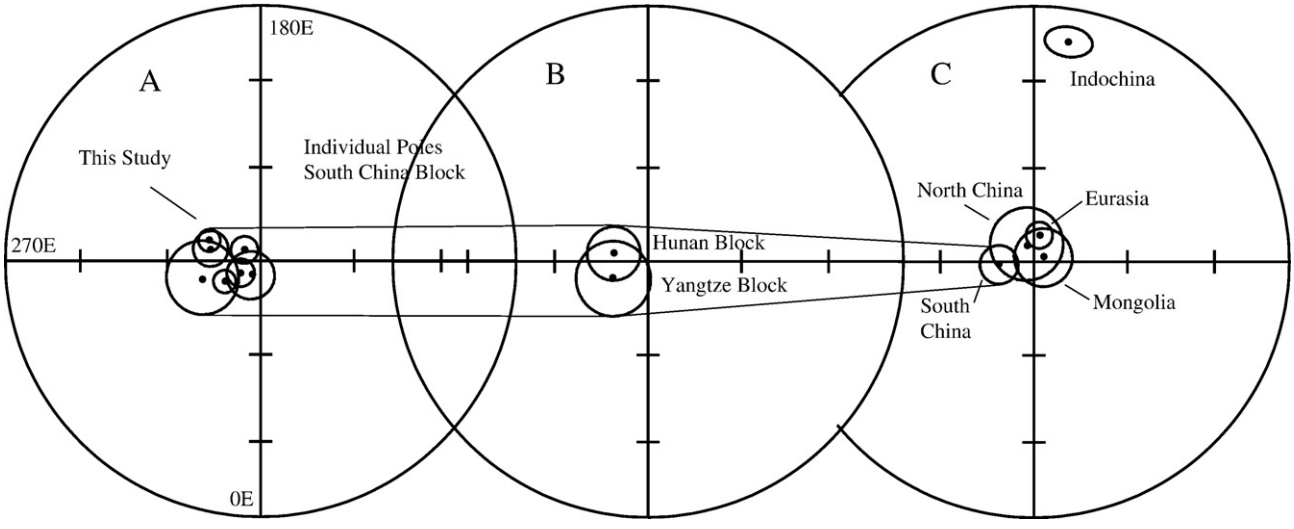

Fig. 7. A series of equal area projections showing average paleomagnetic pole positions (and 95% cones of confidence) for sites on the South China Block (left; Table 1), the Hunan and Yangtze sub-blocks (middle; Table 1), and the major east Asian blocks (right; South China Block – Table 1, Mongolian Block – Zhao et al., 1994, North China Block – Zhao et al., 1994, Indochina – Sato et al., 2001, Eurasia – Besse and Courtillot, 2002). The paleomagnetic pole for Indochina is distinct from those of Mongolia, North China, South China, and Eurasia which overlap.

from Youjiang in Guangxi (Gilder et al., 1993), which is significantly rotated counterclockwise compared to the others, and from the Chuan Dian Fragment in Yunnan (Youshioka et al., 2003), which is significantly rotated clockwise compared to the others, are not included in this comparison since they were locally influenced by large nearby fault systems. The paleomagnetic data from the South China Block suggest that there has been relatively little intra-block vertical axis rotation since the early Tertiary. This result is consistent with Morinaga and Liu (2004) who found good consistency among Cretaceous poles for the SCB outside of those within a 400 km wide swath near the Red River Fault but is different from the results of Gilder et al. (1993) who found poles streaking along a small circle indicating wide-spread intra-block rotations. It seems that any intra-block rotation that may have occurred on the South China Block happened during the late Cretaceous as the early Paleogene data assembled here show no widespread pattern of rotation. Given that the Indian–Asian collision did not take place until the late Paleocene or thereafter (Patriat and Achache, 1984; Beck et al., 1995; Rowley, 1996; Clyde et al., 2003; Aitchison et al., 2007), it is unlikely that any intra-block rotations on the SCB during the Cretaceous are due to this regional tectonic event.

Using the group of well-clustered individual poles for the South China Block, we calculated poles for the Hunan and Yangtze sub-blocks to see if there has been significant relative rotation between the two main terranes that make up the South China Block (Fig. 1; Table 1). This analysis again indicates no significant relative rotation along the broad suture that separates these two terranes (see Hsu et al., 1988; Rowley et al., 1989). We calculated a new early Paleogene pole for the South China Block using the set of well-clustered individual poles (Table 1). Comparing this new pole with early Tertiary poles from adjacent blocks suggest that there has been little relative rotation between the South China Block, North China Block, Mongolia, and 'stable' Eurasia (Fig. 7). By far the most dramatic rotation occurs in the southernmost block of Indochina which has experienced on the order of 70° of clockwise rotation compared to the Eurasian reference pole for the Paleocene (Sato et al., 2001, 2007). These results are inconsistent with those of Sun et al. (2006) who infer the 16.7°±5° of late Cretaceous clockwise rotation in the Hengyang Basin as being in response to the India–Asia collision. This clockwise rotation of the Hengyang Basin, which must have occurred during the late Cretaceous given that the Paleogene data for the same basin show no such rotation, may be related to backarc extension occurring in this area due to the nearby Kula–Pacific subduction zone but is unlikely to be associated with the India–Asia collision given its early timing.

A review of the 'extrusion' model of Asian deformation determined that the northern Asian assemblage (Siberia, Mongolia, North China) has been sutured together since the Cretaceous but that the Q–K–T–J assemblage (Qaidam, Tarim, Kunlun, Junggar) has experienced ~700 km of northward movement with respect to the northern Asian assemblage since that time (Halim et al., 1998). Since the mountains between these assemblages (Altay range and Qilian Shan) are not thought to be extensive enough to account for this convergence, significant strike/slip and rotational movements ('extrusion') are hypothesized to accommodate the observed shortening. The Halim et al. (1998) preferred hypothesis suggests an eastward extrusion of the Mongolia–North China Block-South China Block assemblage along the Mongol–Okhotsk suture in response to the Indian–Asian convergence yet our results indicate no such clockwise rotation. The Indochina block remains the only candidate for significant clockwise rotation caused by Indian indentation. Our results support those of Zhao et al. (1994) who concluded that there was no evidence for first-order rotations in these northern Asian blocks compared to "stable" Eurasia but indicated that second-order rotations may be discovered once sampling was improved.

The SCB early Paleogene pole presented here is somewhat far-sided with respect to the equivalent aged pole for 'stable' Eurasia (Fig. 7). This means that the observed inclinations for South China sites are shallower than expected assuming the Eurasian pole is a reliable comparator. This 'inclination anomaly' has been observed in numerous other paleomagnetic studies of central Asian sediments. These relatively shallow central Asian inclinations have been interpreted to be the results of depositional/compaction processes (Tan et al., 2003; Narumoto et al., 2006; Wang and Yang, 2007), nonrigid Eurasian deformation (Cogne et al., 1999), nondipolar field contributions (Si and Van der Voo, 2001) or to a poorly defined Eurasian pole (Ali and Aitchison, 2006). Studies that have quantified post-depositional inclination shallowing in relevant Asian sediments using rock magnetic procedures have typically found <5° of shallowing due to this mechanism (e.g. Sun et al., 2006) and recent evaluation of Cenozoic basalts from northern blocks also have shallow inclinations suggesting the inclination anomaly is probably not entirely due to depositional or post-depositional inclination shallowing (Hankard et al., 2007).

7. Conclusion

The Chijiang Basin section represents the first section in Asia where faunal, stable isotope, and paleomagnetic data have been integrated into a single stratigraphic record of the Shanghuan–Nongshanian Asian Land Mammal Age boundary. The Shanghuan–Nongshanian boundary coincides with a normal-to-reverse geomagnetic polarity transition and is followed by a gradual ~1.5‰ increase in the mean $\delta^{13}C$ value of organic matter. Correlation of this magnetochemostratigraphic pattern indicates that the polarity reversal likely represents the Chron C27r to C26n boundary and thus correlates closely to the Tiffanian–Torejonian Land Mammal Age boundary in North America. This coincident biotic turnover in far separated ecosystems may share an underlying cause with geochemical changes identified at this time in well-resolved deep sea records; however it is unlike the hyperthermally modulated dispersal event at the PETM in that the turnover occurred mostly in endemic taxa. The paleomagnetic data from Chijiang Basin are also compared to other such results from the South China Block and adjacent blocks to determine the extent of vertical axis rotation since the early Paleogene. Results indicate that the South China Block has experienced very little intra- or inter-block rotation since the early Paleogene compared to these other blocks and stable Eurasia. The Indian–Asian collision seems to have had little rotational effect on the northern assemblage of Asian blocks, compared to the large clockwise rotation observed for the Indochina block to the south.

Acknowledgments

This project was funded by National Geographic Society Grant 7329-02 to Ting, NSF grant EAR0540835 to Clyde, and NSF grant EAR0120727 to Koch. Thanks to Mr. Shuhua Xie of IVPP for his assistance with field work and to Thomas Westerhold for discussion of early Paleocene marine records. Kate Warren and Ben Ho assisted with laboratory measurements. Two anonymous reviews significantly improved the manuscript.

Appendix A. Supplementary data

Supplementary data associated with this article can be found, in the online version, at doi:10.1016/j.epsl.2008.03.009.

References

Aitchison, J.C., Ali, J.R., Davis, A.M., 2007. When and where did India and Asia collide? J. Geophys. Res. 112, B05423. doi:10.1029/2006JB004706.

Ali, J.R., Aitchison, J.C., 2007. Positioning Paleogene Eurasia problem: solution for 60–50 Ma and broader tectonic implications. Earth Planet. Sci. Lett. 251, 148–155. doi:10.1016/j.epsl.2006.09.003.

Archibald, J.D., Gingerich, P.D., Lindsay, E.H., Clemens, W.A., Krause, D.W., Rose, K.D., 1987. First North American Land Mammal Ages in the Cenozoic era. In: Woodburne,

M.O. (Ed.), Cenozoic mammals of North America: geochronology and biostratigraphy. University of California Press, Berkeley, pp. 24–76.
Arens, N.C., Jahren, A.H., Amundson, R., 2000. Can C3 plants faithfully record the carbon isotopic composition of atmospheric carbon dioxide? Paleobiology 26, 137–164.
Beard, K.C., 1998. East of Eden: Asia as an important center of taxonomic origination in mammalian evolution. In: Beard, K.C., Dawson, M.R. (Eds.), Dawn of the Age of Mammals. Bulletin of the Carnegie Museum of Natural History, vol. 34, pp. 5–39.
Beck, R.A., Burbank, D.W., Sercombe, W.J., Riley, G.W., Barndt, J.K., Jurgen, H., Metjle, J., Cheema, A., Shafique, N.A., Lawrence, R.D., Khan, M.A., 1995. Stratigraphic evidence for an early collision between northwest India and Asia. Nature 373, 55–58.
Berggren, W.A., Kent, D.V., Swisher, C.C., Aubry, M.-P., 1995. A revised Cenozoic 622 geochronology and chronostratigraphy. In: Berggren, W.A., Kent, D.V., Aubry, M.-P., Hardenbol, J. (Eds.), Geochronology, Time Scales and Global Stratigraphic Correlation. Society for Sedimentary Geology, Special Publication, vol. 54, pp. 129–212.
Bernaola, G., Baceta, J.I., Orue-Etxebarria, X., Alegret, L., Martin-Rubio, M., Arostegui, J., Dinares-Turell, J., 2007. Evidence of an abrupt environmental disruption during the mid-Paleocene biotic event (Zumaia section, western Pyrenees). Geol. Soc. Amer. Bull. 119, 785–795.
Besse, J., Courtillot, V., 2002. Apparent and true polar wander and the geometry of the geomagnetic field over the last 200 Myr. J. Geophys. Res. 107 (B11). doi:10.1029/2000JB000050.
Bowen, G.J., Clyde, W.C., Koch, P.L., Ting, S., Alroy, J., Tsubamoto, T., Wang, Y., Wang, Y., 2002. Mammalian dispersal at the Paleocene/Eocene boundary. Science 295, 2062–2065.
Bowen, G.J., Koch, P.L., Meng, J., Ye, J., Ting, S., 2005. Age and correlation of fossiliferous late Paleocene–early Eocene strata of the Erlian Basin, Inner Mongolia, China. Am. Mus. Novit. 3474, 1026.
Bralower, T.J., Premoli Silva, I., Malone, M.J., 2006. Leg 198 synthesis: a remarkable 120-m.y. record of climate and oceanography from Shatsky Rise, northwest Pacific Ocean. In: Bralower, T.J., Premoli Silva, I., Malone, M.J. (Eds.), Proceedings of the Ocean Drilling Program. Scientific Results, vol. 198.
Butler, R.F., Krause, D.W., Gingerich, P.D., 1987. Magnetic polarity stratigraphy and biostratigraphy of middle-late Paleocene continental deposits of south-central Montana. J. Geol. 97, 647–657.
Clyde, W.C., Gingerich, P.D., 1998. Mammalian community response to the latest Paleocene thermal maximum: an isotaphonomic study in the northern Bighorn Basin, Wyoming. Geology 26, 1011–1014.
Clyde, W.C., Khan, I.H., Gingerich, P.D., 2003. Stratigraphic response and mammalian dispersal from initial India–Asia collision: evidence from the Ghazij Formation, Balochistan, Pakistan. Geology 31, 1097–1100.
Clyde, W.C., Hamzi, W., Finarelli, J.A., Wing, S.L., Schankler, D., Chew, A., 2007. Basin-wide magnetostratigraphic framework for the Bighorn Basin, Wyoming. Geol. Soc. Amer. Bull. 119, 848–859.
Cogne, J.P., Halim, N., Chen, Y., Courtillot, V., 1999. Resolving the problem of shallow magnetization of the Tertiary age in Asia: insights from paleomagnetic data from the Qiangtang, Kunlun, and Qaidam blocks (Tibet, China), and a new hypothesis. J. Geophys. Res. 17, 715–734.
Enkin, R.J., Courtillot, V., Xing, L., Zhang, Z., Zhuang, Z., Zhang, J., 1991. The stationary Cretaceous paleomagnetic pole of Sichuan (South China Block). Tectonics 10, 547–559.
Enkin, R.J., Yang, Z., Chen, Y., Courtillot, V., 1992. Paleomagnetic constraints on the geodynamic history of the major blocks of China from the Permian to the present. J. Geophys. Res. 97, 13953–13989.
Fisher, R.A., 1953. Dispersion on a sphere. Proc. R. Soc. (Lond.) A217, 295–305.
Gilder, S.A., Coe, R.S., Wu, H., Kuang, G., Zhao, X., Wu, Q., Tang, X., 1993. Cretaceous and Tertiary paleomagnetic results from southeast China and their tectonic implications. Earth Planet. Sci. Lett. 117, 637–652.
Gingerich, P.D., 1989. New earliest Wasatchian mammalian fauna from the Eocene of northwestern Wyoming: composition and diversity in a rarely sampled high-floodplain assemblage. Univ. Mich. Pap. Paleontol. 28, 1–97.
Gingerich, P.D., 1995. Mammalian responses to climate change at the Paleocene–Eocene boundary: Polecat Bench record in the northern Bighorn Basin, Wyoming. In: Wing, S.L., Gingerich, P.D., Schmitz, B., Thomas, E. (Eds.), Causes and Consequences of Globally Warm Climates in the Early Paleogene. Geological Society of America, Special Paper, vol. 369, pp. 463–478. Boulder, CO.
Gradstein, F.M., Ogg, J.G., Smith, A.G., et al., 2004. Geological Time Scale 2004. Cambridge University Press, Cambridge.
Halim, N., Cogne, J.P., Chen, Y., Atasiei, R., Besse, J., Courtillot, V., Gilder, S., Marcoux, J., Zhao, R.L., 1998. New Cretaceous and early Tertiary paleomagnetic results from Xining–Lanzhou basin, Kunlun and Qiangtang blocks, China: implications on the geodynamic evolution of Asia. J. Geophys. Res. 103, 21,025–21,045.
Hankard, F., Cogne, J.-P., Kravchinsky, V.A., Carporzen, L., Bayasgalan, A., Lkhagvadorj, P., 2007. New Tertiary paleomagnetic poles from Mongolia and Siberia at 40, 30, 20, and 13 Ma: clues on the inclination shallowing problem in central Asia. J. Geophys. Res. 112.
Higgins, P., 2003. A Wyoming succession of Paleocene mammal-bearing localities bracketing the boundary between the Torrejonian and Tiffanian North American Land Mammal "Ages". Rocky Mt. Geol. 38, 247–280.
Hooker, J.J., 1998. Mammalian faunal change across the Paleocene–Eocene transition in Europe. In: Aubry, M.-P., Lucas, S.G., Berggren, W.A. (Eds.), Late Paleocene–early Eocene Climatic and Biotic Events in the Marine and Terrestrial Records. Columbia University Press, New York, pp. 419–441.
Hsu, K.J., Shu, S., Jiliang, L., Haihong, C., Haipo, P., Sengor, A.M.C., 1988. Mesozoic overthrust tectonics in south China. Geology 16, 418–421.
Huang, K., Opdyke, N.D., 1992. Paleomagnetism of Cretaceous to lower Tertiary rocks from southwestern Sichuan: a revisit. Earth Planet. Sci. Lett. 112, 29–40.
Huang, B., Piper, J.D.A., Zhang, C., Li, Z., Zhu, R., 2007. Paleomagnetism of Cretaceous rocks in the Jiaodong Peninsula, eastern China: insight into block rotations and neotectonic deformation in eastern Asia. J. Geophys. Res. 112, B03106. doi:10.1029/2006JB004462.
Kent, D.V., Xu, G., Huang, K., Zhang, W.Y., Opdyke, N.D., 1986. Paleomagnetism of upper Cretaceous rocks from South China. Earth Planet. Sci. Lett. 79, 179–184.
Koch, P.L., Zachos, J.C., Gingerich, P.D., 1992. Correlation between isotope records in marine and continental carbon reservoirs near the Palaeocene/Eocene boundary. Nature 358, 319–322.
Koch, P.L., Clyde, W.C., Hepple, R.P., Fogel, M.L., Wing, S.L., Zachos, J.C., 2003. Carbon and oxygen isotope records from paleosols spanning the Paleocene–Eocene boundary, Bighorn Basin, Wyoming. In: Wing, S.L., Gingerich, P.D., Schmitz, B., Thomas, E. (Eds.), Causes and Consequences of GloballyWarm Climates in the Early Paleogene. Geological Society of America, Special Paper, vol. 369, pp. 49–64. Boulder, CO.
Li, C.K., Ting, S.Y., 1983. The Paleogene mammals of China. Bulletin of the Carnegie Museum of Natural History, vol. 21.
Lofgren, D.L., Lillegraven, J.A., Clemens, W.A., Gingerich, P.D., Williamson, T.E., 2004. Paleocene biochronology of North America: the Puercan through Clarkforkian land mammal ages. In: Woodburne, M.O. (Ed.), Late Cretaceous and Cenozoic mammals of North America: biostratigraphy and geochronology. Columbia University Press, New York, pp. 43–105.
Lourens, L.J., Sluijs, A., Kroon, D., Zachos, J.C., Thomas, E., Rohl, U., Bowles, J., Raffi, I., 2005. Astronomical pacing of late Palaeocene to early Eocene global warming events. Nature 435, 1083–1087.
Molnar, P., Tapponnier, P., 1975. Cenozoic tectonics of Asia: effects of a continental collision. Science 189, 419–426.
Morinaga, H., Liu, Y., 2004. Cretaceous paleomagnetism of the eastern South China Block: establishment of the stable body of SCB. Earth Planet. Sci. Lett. 222, 971–988.
Narumoto, K., Yang, Z., Takemoto, K., Zaman, H., Morinaga, H., Otofuji1, Y., 2006. Anomalously shallow inclination in middle-northern part of the South China block: palaeomagnetic study of Late Cretaceous red beds from Yichang area. Geophys. J. Int. 164, 290–300.
O'Leary, M.H., 1995. Environmental effects on carbon isotope fractionation in terrestrial plants. In: Wada, E., et al. (Ed.), Stable Isotopes in the Biosphere. Kyoto Univ. Press, Kyoto, pp. 78–91.
Patriat, P., Achache, J., 1984. India–Eurasia collision chronology has implications for crustal shortening and driving mechanism of plates. Nature 311, 615–621.
Qizhong, L., Shen, D., Ruiyan, Y., Zelin, N., 1986. A case study of the Eocene paleomagnetic pole sites and characteristics of magnetic strata in eastern Yunnan, China. Geol. Res. South China Sea 32, 144–149.
Quillevere, F., Aubry, M.-P., Norris, R.D., Berggren, W.A., 2002. Paleocene oceanography of the eastern subtropical Indian Ocean: an integrated magnetobiostratigraphic and stable isotope study of ODP Hole 761B (Wombat Plateau). Palaeogeogr. Palaeoclimatol. Palaeoecol. 184, 371–405.
Ren, J., Tamaki, K., Li, S., Zhang, J., 2002. Late Mesozoic and Cenozoic rifting and its dynamic setting in eastern China and adjacent areas. Tectonophysics 344, 175–205.
Romer, A.S., 1966. Vertebrate Paleontology, Third Edition. University of Chicago Press, Chicago.
Rowley, D.B., 1996. Age of initiation of collision between India and Asia: a review of the stratigraphic data. Earth Planet. Sci. Lett. 145, 1–13.
Rowley, D.B., Ziegler, A.M., Gyou, N., 1989. Comment on Mesozoic overthrust tectonics in south China. Geology 17, 384–386.
Russell, D.E., Zhai, R., 1987. The Paleogene of Asia: mammals and stratigraphy. Mém. Mus. Natl. d'Hist. Nat., Sér. C 52, 1–488 Paris.
Sato, K., Liu, Y., Zhu, Z., Yang, Z., Otofuji, Y., 2001. Tertiary paleomagnetic data from northwestern Yunnan, China: further evidence for large clockwise rotation of the Indochina block and its tectonic implications. Earth Planet. Sci. Lett. 185, 185–198.
Sato, K., Liu, Y.Y., Wang, Y.B., Yokoyama, M., Yoshioka, S., Yang, Z., Otofuji, Y.I., 2007. Paleomagnetic study of Cretaceous rocks from Pu'er, western Yunnan, China: evidence of internal deformation of the Indochina block. Earth Planet. Sci. Lett. 258, 1–15.
Si, J., Van der Voo, R., 2001. Too-low magnetic inclinations in central Asia: an indication of long-term Tertiary non-dipole field? Terra Nova 13, 471–478.
Still, C.J., Berry, J.A., Collatz, G.J., DeFries, R.S., 2003. Global distribution of C-3 and C-4 vegetation: carbon cycle implications. Glob. Biogeochem. Cycles 17, 1006.
Sun, Z., Yang, Z., Yang, T., Pei, J., Yu, Q., 2006. New Late Cretaceous and Paleogene paleomagnetic results from south China and their geodynamic implications. J. Geophys. Res. 111, B03101. doi:10.1029/2004JB003455.
Szalay, F.S., McKenna, M.C., 1971. Beginning of the age of mammals in Asia: the late Paleocene Gashato fauna, Mongolia. Bull. Am. Mus. Nat. Hist. 144, 273–314.
Tan, X., Kodama, K.P., Chen, H., Fang, D., Sun, D., Li, Y., 2003. Paleomagnetism and magnetic anisotropy of Cretaceous red beds from the Tarim basin, northwest China: evidence for a rock magnetic cause of anomalously shallow paleomagnetic inclinations from central Asia. J. Geophys. Res. 108, 2107.
Tapponnier, P., Peltzer, G., Le Dain, A.Y., Armijo, R., Cobbold, P., 1982. Propagating extrusion tectonics in Asia: new insights from simple experiments with plasticine. Geology 10, 611–616.
Tauxe, L., 1998. Paleomagnetic Principles and Practice. Kluwer, Netherlands.
Taylor, B., Hayes, D.E., 1983. Origin and history of the South China Sea basin. In: Hayes, D.E. (Ed.), The Tectonic and Geologic Evolution of Southeast Asian Seas and Islands, Part 2. AGU Geophysical Monograph, vol. 27, pp. 23–56.
Ting, S., 1998. Paleocene and early Eocene land mammal ages of Asia. In: Beard, K.C., Dawson, M.R. (Eds.), Dawn of the Age of Mammals in Asia. Bulletin of Carnegie Museum of Natural History, vol. 34, pp. 124–147.
Ting, S., Meng, J., Li, Q., Wang, Y., Tong, Y., Schiebout, J.A., Koch, P.L., Clyde, W.C., Bowen, G.J., 2007. *Ganungulatum xincunliense*, an artiodactyl-like mammal (Ungulata,

Mammalia) from the Paleocene, Chijiang Basin, Jiangxi, China. Vertebr. PalAsiatica 10, 278–286.
Tong, Y., 1979a. Some Eocene uintathere materials of Chijiang Basin, Jiangxi. Mesozoic and Cenozoic Red Beds of South China. Science Press, Beijing, pp. 395–399.
Tong, Y., 1979b. The new materials of archaeolambdids from South Jiangxi. Mesozoic and Cenozoic Red Beds of South China. Science Press, Beijing, pp. 377–381.
Tong, Y., 1979c. A late Paleocene primate from South China. Vertebr. PalAsiatica 17, 65–70.
Tong, Y., Huang, X., 1986. New arctostylopids (Notoungulata, Mammalia) from the late Paleocene of Jiangxi. Vertebr. PalAsiatica 24, 121–128.
Tong, Y., Zhang, Y., Wang, B., Ding, S., 1976. The lower Tertiary of the Nanxiong and Chijiang basins. Vertebr. PalAsiatica 14, 16–25.
Tong, Y., Zhang, Y., Zheng, J., Wang, B., Ding, S., 1979. The discussion of the lower Tertiary strata and mammalian fauna of Chijiang basin, Jiangxi. Mesozoic and Cenozoic Red Beds of South China. Science Press, Beijing, pp. 400–406.
Tong, Y., Zheng, S., Qiu, Z., 1995. Cenozoic mammal ages of China. Vertebr. PalAsiatica 33, 290–314.
Wang, B., Yang, Z., 2007. Late Cretaceous paleomagnetic results from southeastern China, and their geological implication. Earth Planet. Sci. Lett. 258, 315–333.
Wang, Y., Hu, Y., Chow, M., Li, C., 1998. Chinese Paleocene mammal faunas and their correlation. In: Beard, K.C., Dawson, M.R. (Eds.), Dawn of the Age of Mammals in Asia. Bulletin of Carnegie Museum of Natural History, vol. 34, pp. 89–123.
Watson, G.S., 1956. A test for randomness of directions. Mon. Not. R. Astron. Soc. Geophys. Suppl. 7, 160–161.
Westerhold, T., Rohl, U., Raffi, I., Fornaciari, Eliana, Monechi, S., Reale, V., Bowles, J., Evans, H.F., 2007. Astronomical calibration of the Paleocene time. Palaeogeogr. Palaeoclimatol. Palaeoecol. doi:10.1016/j.palaeo.2007.09.016 vol.
Woodburne, M.O., Swisher, C.C., 1995. Land mammal high-resolution geochronology, intercontinental overland dispersals, sea level, climate, and vicariance. In: Berggren, W.A., Kent, D.V., Aubry, M.-P., Hardenbol, J. (Eds.), Geochronology, Time Scales and Global Stratigraphic Correlation. SEPM Spec. Pub., vol. 54, pp. 335–364.
Xu, J.W., Zhu, G., Tong, W.X., Cui, K.R., Liu, Q., 1987. Formation and evolution of the Tancheng–Luijiang wrench fault system: a major shear system to the northwest of the Pacific Ocean. Tectonophysics 134, 273–310.
Yoshioka, S., Liub, Y.Y., Satoa, K., Inokuchic, H., Sua, L., Zamana, H., Otofujia, Y., 2003. Paleomagnetic evidence for post-Cretaceous internal deformation of the Chuan Dian Fragment in the Yangtze block: a consequence of indentation of India into Asia. Tectonophysics 376, 61–74.
Zachos, J.C., Pagani, M., Sloan, L., Thomas, E., Billups, K., 2001. Trends, rhythms, and aberrations in global climate 65 Ma to Present. Science 292, 686–693.
Zachos, J.C., Kroon, D., 25 others, 2004. Early Cenozoic extreme climates: the Walvis Ridge transect. Proceedings of the Ocean Drilling Program. Leg 208. http://www-odp.tamu.edu/publications/208-IR/208ir.htm.
Zhang, Zh.M., Liou, J.G., Coleman, R.G., 1984. An outline of the plate tectonics of China. Geol. Soc. Amer. Bull. 95, 295–312.
Zhao, A., Te, J., Li, H., Zhao, Z., Tan, Z., 1991. Extinction of the dinosaurs across the Cretaceous–Tertiary boundary in Nanxiong Basin, Guangdong Province. Vertebr. PalAsiatica 29, 1–20.
Zhao, X., Coe, R., Zhou, Y., Hu, S., Wu, H., Kuang, G., Dong, Z., Wang, J., 1994. Tertiary paleomagnetism of North and South China and reappraisal of late Mesozoic paleomagnetic data from Eurasia: implications for the Cenozoic tectonic history of Asia. Tectonophysics 235, 181–203.
Zheng, J., Tong, Y., Ji, H., Zhang, F., 1973. The subdivision of the “Red Beds” of Chijiang Basin, Jiangxi. Vertebr. PalAsiatica 11, 206–211.